MECHANICAL BEHAVIOR OF SLS COMPONENTS IN RELATION TO THE BUILD ORIENTATION DURING THE SINTERING PROCESS AS MEASURED BY ESPI

Felipe Amado-Becker, Ricardo A. Díaz, Jorge Ramos-Grez[1]

Mechanical and Metallurgical Engineering Department,
Pontificia Universidad Católica de Chile
Av. Vicuña Mackenna 4860 - Macul - Santiago - CHILE

Abstract

Selective Laser Sintering (SLS) allows producing real parts from CAD data from materials with different characteristics compared to the final model, presenting dissimilar mechanical properties between the prototype and the product. The purpose of this work is to correlate the mechanical behavior of beam-type specimens produced by SLS with build orientation angle used as a process parameter, also attempting to demonstrate how this parameter affects the accuracy of the Empirical Similitude Method (ESM). ESM presents itself as a valuable tool when creating scale models with SLS, specifically in the framework of evolutionary product design. More specifically, the Young modulus variation of test specimens of well-known dimensions and material (Duraform™ PA[2]), will be characterized by loading them within the elastic range. The resulting elastic deformations will be measured using the technique of Electronic Speckle Pattern Interferometry (ESPI) for small deformations in an out-of-plane configuration, contrasting these results with the elastic theory of deformations. As a main result, it was found that there exists a linear correlation between the build angle and the elastic modulus of the parts. Secondly, it was demonstrated empirically that the ESM predicts better the mechanical response of the part than TSM. Moreover, a 30% error reduction can be achieved within the ESM when using the build orientation angle as a process parameter.

Introduction

Product design processes increasingly make use of rapid prototyping technologies, primarily because of the reported development-cost-reduction benefits [2]. RP models offer unbalanced advantages in freeform fabrication especially if the reduced timeframe required for obtaining an actual physical model is taken into consideration.

A feature of most RP technologies is that their processes depend heavily on layered manufacturing. This results in the fact that build orientation plays a role in the mechanical properties of the model. This paper explores the effects observed in beams fabricated via SLS. In this technology polymeric powder (Duraform™ PA) is sintered layer-by-layer, so the created model can be characterized by a transverse isotropic behavior, with its Young modulus equal in both directions contained in the build plane. Out-of-plane deflections within elastic range of these beams can be then measured using Electronic Speckle Pattern Interferometry (ESPI). This technique consists in illuminating a diffuse object by a coherent beam of radiation (a visible laser

---

[1] Corresponding author: jramos@ing.puc.cl
[2] Duraform™ PA process conditions on material's data sheet.

beam) to produce a grainy structure in space over the studied surface known as the speckle pattern. As the beam-type specimen deflects due to loading, a change in phase takes place, and consequently, a change in irradiance as well. Using electronic detection and digital subtraction from a reference image, fringes linked to the displacements arise. With a simple relationship, these fringes provide the deflection profile of the beam. Complementing the measurements with the elastic theory, more particularly with the uniform beam deflection equation, Young modulus can be obtained. Young modulus values will be compared for beams built in four different orientations (0°, 30°, 60° and 90°).

It is important to emphasize that a model produced via SLS has capabilities that enable adequate use for product evaluation purposes such as fit and form and more limited, to evaluate function. So, determination of model's Young modulus is important in function evaluation.

Finally, in order to solve the problem of dissimilar mechanical properties between the prototype and the desired product, and taking into account the limitations inherent to technologies and availability of materials employed, similitude techniques have been developed to correlate prototype behavior with the final product's mechanical properties [3]. The results obtained will allow evaluation of how build angle affects the Traditional Similitude Method (TSM) and Empirical Similitude Method (ESM) described in the cited reference.

Fabrication of specimens via SLS and ESPI measurements of displacements

Fabrication of specimens

All specimens were built using a DTM SLS-125 Beta machine in a single run to avoid possible distortions associated with temperature variations when sintered independently. Laser power was set at 6 W (at the surface of the powder) for the entire sintering process in a standard atmosphere. The scanning parameters were set at ss = 50 and sp = 270. Sintered layers had a thickness equal to 0,005 in. Product family specimens correspond to aluminum beams.

The sintered specimens where grouped in two sets. The first one consisted of four uniform beams with build orientation of 0º, 30º, 60º and 90º (Figure 1). The second set included two beams built with only a 0º and 90º orientations, however, having different shape (four cylindrical bores along the main axis) with respect to the previous models, as shown in Figure 2. These two beams where employed for testing and evaluating the effect of orientation on similitude techniques. Beam dimensions are displayed in Figure 3.
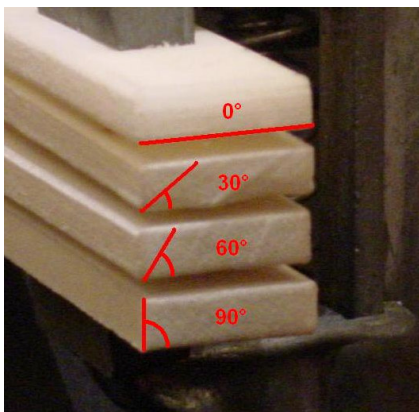

Figure 1: Sintered beams with different build orientation (cross-section)
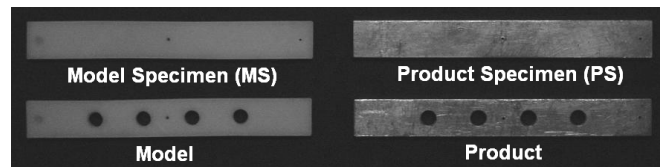

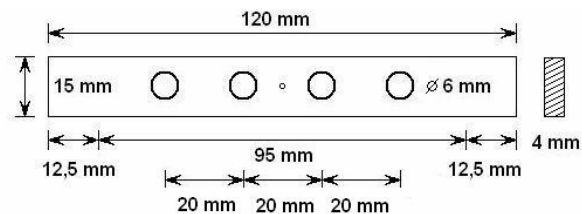**Figure 2: Change in shape (product evolution)**

Figure 3: Beam dimensions

ESPI measurements of displacements

Both beams free end where clamped, so a fixed support configuration was achieved. Load was applied at the center in five incremental weights following a similar procedure as the one described in [5]. Experimental setup for beam loading is shown in Figure 4. A ball bearing was used to avoid bias on load conditions due the relative important friction magnitude when working with small weights.

Measurements of beam deformation can be obtained through a number of techniques, but ESPI offers the advantage of acquiring the whole deflection field along the beam with high accuracy. However, this requires small loadings, a

Figure 4: Beam loading setup

helpful requirement since it allows results within the elastic domain. This is fundamental for modulus calculation afterwards as well as for avoiding large deflections coupled with geometric distortions that result in variations in the effective value of the Young's modulus [4].

A Mach-Zehnder interferometer was used. It consists of a coherent laser beam divided into two collimated optical paths that converge and illuminate the studied object's surface. When the specimen is loaded, a change in the optical path length occurs and, when compared to a reference initial state, the intensity of the resulting pattern can be associated with displacements.

Acquiring this pattern electronically using a digital camera and subtracting it from the reference image by means of processing software (Optofringe), results in an image showing interference fringes. This image is displayed in real time on the computer screen.

According to Sirohi [5], the fringes represent out-of-plane displacements that can be obtained by the following relationship:

$$\delta = N \cdot \frac{\lambda}{2}. \quad (1)$$

Where δ is displacement, N the fringe number (integer number) and $\lambda = 632{,}8$ nm is the wavelength of the illuminating low power He-Ne laser. Equation (1) demonstrates that the arrangement offers a sensitivity of half a wavelength. Interferometer setup and a sample fringe image are shown in Figures 5 and 6.
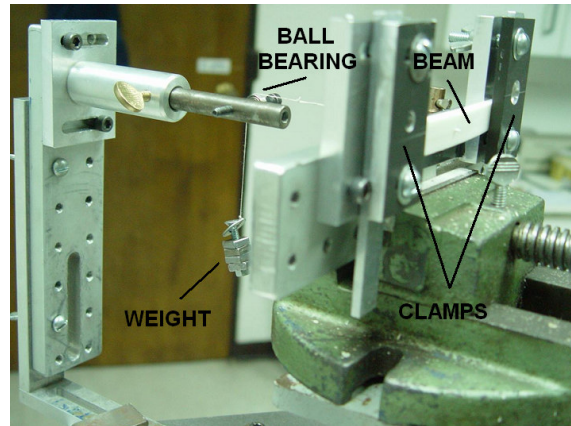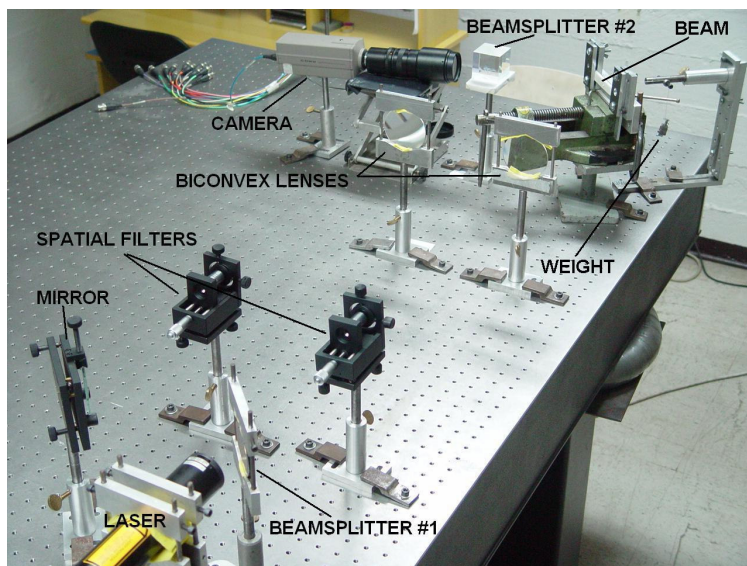

Figure 5: Mach-Zehnder setup for beam deflection measurements via ESPI

The next step is to relate each fringe's center to its position over the beam for which a reference scale is placed alongside. Due to symmetry of the loading conditions along the beam length, only half of it is considered for analysis.

A set of out-of-plane coordinates is obtained and a cubic data fit is performed. The polynomial coefficients values are then associated with the analytical expressions of the elastic uniform beam deflection equations [6]. For each loading case (5 per beam), two elastic modulus are obtained and an average modulus for each beam is calculated. Equations describing the related phenomena are presented below.
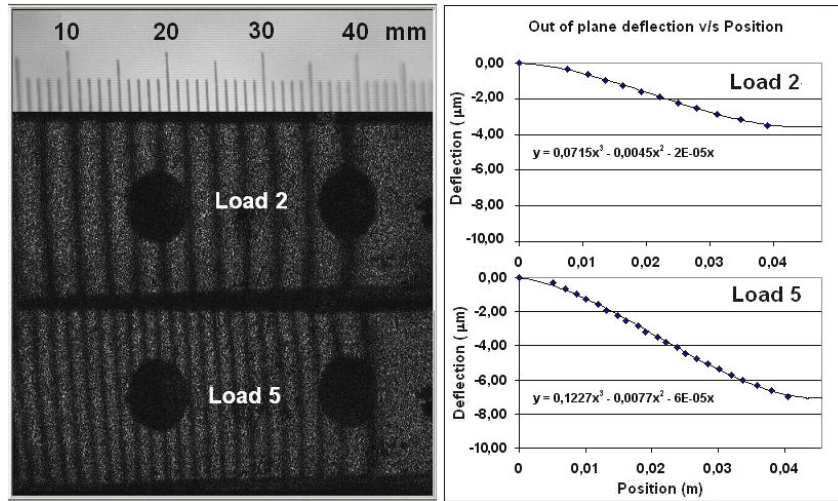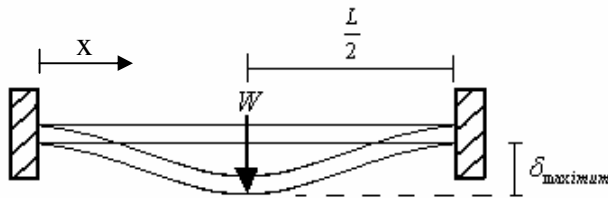

Figure 6: Interference fringes and its deformation profile

$$\delta = \frac{W}{48EI}(4x^3 - 3Lx^2) \quad \text{for } 0 < \text{x} < \frac{L}{2}. \quad (2)$$

$$\text{where, } \delta_{max\,imum} = \frac{WL^3}{192EI} \quad \text{at x} = \frac{L}{2}. \quad (3)$$

Additionally, using the same technique, Young modulus for aluminum beams could be measured. A 7 % difference from nominal value (70 GPa) was determined ($E_{measured}$ = 74,6 GPa). This result reveals the high accuracy of the procedure previously described.

Traditional and Empirical Similitude Techniques

Functional evaluation with rapid prototypes as predictors of the mechanical behavior for final products is a field of study where contributions are yet to be made. Dimensional analysis provides the basis for TSM and ESM. TSM is characterized by definition of constant scale factors used for correlating behavior between two systems [4]. Due to the objective of material characterization of this work, physical dimensions among all the specimens remain invariant, generating constant and equal scale factors. Only the ratio between the product and model specimens' nominal Young moduli is considered for scaling loads applied to the product family. Using nominal data provided by manufacturers, this factor reaches a value of 43,75 (E_{alum} / $E_{Duraform\ PA}$ = 70 GPa / 1,6 GPa). ESM uses additional information from empirical testing, considering distortions among specimens. This method requires more effort than TSM, resulting in average error reduction. Correlations for shape and scale changes are represented by transformation matrices F and S as described by Cho [1].

724

Results and Discussion

Linear relationship between elastic modulus and build angle

When analyzing the obtained results from the first set of specimens, it can be appreciated that a variation in the mechanical behavior exists, characterized by a linear correlation between the build angle and the elastic modulus of the material. As the build angle is increased, the elastic modulus diminishes. The nominal value according to material's technical data (Duraform™ PA) corresponds to 1,60 GPa. Taking this as reference, the maximum percent variation is obtained for an angle of 0° with a value of 19%. This behavior can be explained due to the transverse isotropic material property, which varies in relation to the isotropic orientation plane (changes in transverse shear modulus). Further studies of shear modulus values between layers will be conducted.
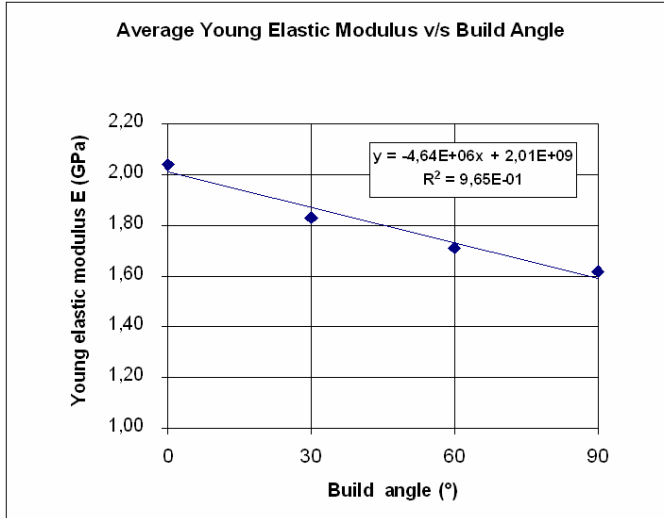

Figure 7: Linear data fit for elastic modulus variation

Building angle (Deg.)	Young elastic modulus E (GPa)	Variation from nominal value 1,60 GPa (%)
0°	2,04	19
30°	1,83	10
60°	1,71	5
90°	1,61	1

Table 1

Build angle relevance in TSM and ESM

On the other hand, when evaluating both sets of specimens (but only specimens built at 0° and 90° orientation) through TSM and ESM, appreciable differences in TSM can be obtained (see Table 2). The average error for TSM at 0° orientation corresponds to a maximum value of 41%, which is reduced to 22% as the build angle
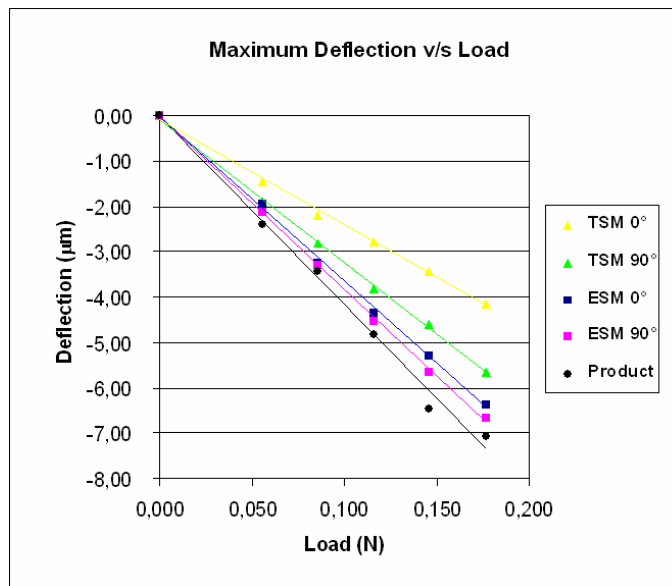
Figure 8: Similitude methods comparison v/s orientation

	Error Analysis (%)			
Load (N)	ESM 0°	TSM 0°	ESM 90°	TSM 90°
0,055	19	39	11	21
0,085	5	36	4	18
0,116	10	42	6	21
0,146	18	47	12	29
0,176	10	41	6	20
Average	12	41	8	22

Table 2

iincreases until reaching 90°. This suggests that build orientation can change the average porcentage error in as much as a 19%.

In the case of ESM, as theory predicts, the adjustment to the final product is still more precise than TSM. A 12% error is obtained for the 0° build orientation model while an 8% error is achived for the 90° build orientation one. In other words, a 30% error reduction in the ESM has been obtained. Moreover, even when considerable material distortions are present (in this case a Young modulus variation of 19%), ESM precision practically remains invariant (4%) when compared with the TSM (19%). It must be emphasized that the ESM precision variation in relation to the build orientation is also reduced as the elastic modulus reaches the nominal Young modulus value of the model material.

Conclusions

Material's mechanical behavior was characterized through the Young modulus variation measurements in relation to the build orientation angle during the selective laser sintering process. As the build orientation angle is increased, the elastic modulus of the part diminishes. The maximum registered dissimilarity corresponds to a 19% with respect to the nominal value 1,60 GPa.

Secondly, the error reduction characteristic of ESM was corroborated in an empirical way when material distortions are present. The average error difference between the two build orientations obtained by the ESM is smaller than the one obtained by TSM.

This error can also be minimized as the material nominal elastic modulus (real) is approached.

To accomplish these latter goals, ESPI technique was used allowing measuring the complete deformation field of the specimens in study, obtaining the deflection profile for each beam and set of loads. This allows making a more precise adjustment at the time of obtaining the maximum deflection. Also it would allow evaluating variations in any other point of interest.

Finally it is important to indicate that the selective laser sintering of the prototypes (model and model specimen) must be carried out in the same build orientation, since otherwise distortions in the F matrix are induced. The latter matrix only incorporate shape dissimilarities and not material distortions between the model and the model specimen (i.e., S and F are independent matrices).

Acknowledgements

References

[1] Cho, U., Wood, K.L. and Crawford, R.H. (1998), "Online functional testing with rapid prototypes: a novel empirical similarity method", Rapid Prototyping Journal, Volume 4, Number 3, pp. 128-138.

[2] Dulieu-Barton, J.M. and Fulton, M.C. (2000), "Mechanical properties of a typical stereolithograhy resin", *Strain*, Volume 36, Number 2, pp. 81-7.

[3] Dustin, A.J., Wood, K.L. (2005), "Using rapid prototypes for functional evaluation of evolutionary product designs," Rapid Prototyping Journal, Volume 11, Number 3, pp. 125-131.

[4] Dutson, A.J. (2002), "Functional prototyping through advanced similitude techniques", Doctoral Dissertation, The University of Texas, Austin, TX.

[5] Sirohi, R.S. (1993), *Speckle Metrology*, Marcel Dekker, New York, pp. 99-125.

[6] Timoshenko, S.P. and Gere, J.M. (1961), *Theory of Elastic Stability*, 2nd Edition, McGraw-Hill, New York, NY.

[7] DuraForm™ PA and GF plastic data sheet (2005), 3D Systems Corporation.